On the presence or absence of geminal Si···N interactions (α-effect) in pentafluorophenylsilyl compounds with SiCN, SiNN and SiON backbones†

Markus Woski, Raphael J. F. Berger and Norbert W. Mitzel*

Received 19th May 2008, Accepted 11th July 2008
First published as an Advance Article on the web 8th September 2008
DOI: 10.1039/b808388f

The silanes $C_6F_5SiF_2CH_2NMe_2$ (**1**), $C_6F_5SiF_2N(SiMe_3)NMe_2$ (**2**) and $C_6F_5SiF_2ONMe_2$ (**3**) with pentafluorophenyl substituents and geminal N atoms have been prepared by the reaction of $C_6F_5SiF_3$ with $LiCH_2NMe_2$, $LiN(SiMe_3)NMe_2$ and $LiONMe_2$, respectively. The compounds have been characterised by spectroscopic methods and crystal structure determination. Comparison of measured and calculated IR spectra has provided insight into the conformational composition of the vapour of **3**. Whereas **2** and **3** show interactions between the geminal Si and N atoms, **1** does not. Further analysis of the bonding situation has been undertaken by quantum chemical calculations of the rotation and bending potentials of the $C_6F_5SiF_2$–X–NMe_2 units.

Introduction

The last 40 years have seen many debates about the so called α-effect in silicon chemistry. This was initially deduced from reduced basicities of α-silylated (germylated and stannylated) amines as compared to alkylated ones.[1] The reason for this effect was discussed in terms of the postulate of a dative bond between the nitrogen and the silicon atom, *i.e.* the acceptor quality of silicon reducing in this way the N basicity. It should be noted, that the term "α-effect" is also used in a different context in silicon chemistry to describe the stabilisation of α-carbanions by silyl groups;[2] these concepts should not be confused.

Many additional properties of α-silylated amines and other geminal systems such as magnetic susceptibility, dipole moments,[3] various spectroscopic parameters[4] and structural parameters[5] have since then been attributed to the α-effect. The higher reactivity of the silicon atom in such compounds is manifest from the uncommon ease of cleavage of the Si–C(N) bond[6] and from the observed increased reaction speed towards substitution reactions at Si. The latter effect has found widespread application in the chemistry of organofunctional silanes and led to the development of the so called α-silanes, which are nowadays employed as surface mediators, adhesion promoters and generally as covalent linkers between the inorganic and organic parts of composite materials.[7]

Despite this, the α-effect is not really well understood in terms of its electronic details. We have shown that there are classes of compounds with Si–X–N backbones (X = spacer group), clearly featuring an attractive force between the Si and N atoms. This holds true for X = O and N, *i.e.* the *O*-silylhydroxylamines[8] and -oximes[9] and the silylhydrazines.[10] The examples with the most pronounced of such interactions are compounds displaying the feature of a three-membered SiXN ring with short Si···N distances and small Si–X–N angles. Such examples include $ClH_2SiONMe_2$,[11] $F_3SiONMe_2$[12] and $(F_3C)F_2SiONMe_2$[13] for the hydroxylamines and $F_3SiN(SiMe_3)NMe_2$[14] for the hydrazines. Despite the many structural parameters determined in the solid and the gas phase, the Si···N interaction remained difficult to describe, as only very little electron density is found between Si and N atoms. In electron density topologies analysed in terms of the quantum theory of atom in molecules (QTAIM) no bond critical points for the Si···N interactions are found.[13] Moreover, sophisticated levels of theory are necessary for a correct reproduction of experimental findings.[15] In the gas phase $F_3SiCH_2NMe_2$ has an 110.3(7)° Si–C–N angle (gas electron diffraction), not at all indicating an attractive Si···N interaction[16] [as also found in $H_3SiCH_2NMe_2$, angle Si–C–N 114.7(3)°].[17] By contrast to this and the monomeric nature of all SiON and SiNN compounds studied in the solid state so far, $F_3SiCH_2NMe_2$ is a dimer with two intermolecular N→Si dative bonds in a six-membered $Si_2N_2C_2$ ring in its crystals. It adopts even widened Si–C–N angles of 120.3(1) and 120.4(1)° in the crystalline phase.[16]

In contrast to SiON and SiNN backbones, no example for the SiCN compounds has been found so far, which shows the described features of small Si–C–N angles or short Si···N distances. This was surprising as these are exactly those compounds for which an "α-effect" is claimed and found to be active, but obviously has a different origin than that proposed in the original postulate.

Instead of intriguing structural features, $F_3SiCH_2NMe_2$ has an unexpectedly flat bending potential for the SiCN unit and a charge distribution inconsistent with the picture of a classical Si···N interaction.[16]

In this contribution we present a set of pentafluorophenylsilanes with SiON, SiNN and SiCN backbones, which allows for the first time a consistent comparative study of the ground state structures of a series of compounds monomeric in the solid state and with the same substitution pattern at the silicon atom.

Results and discussion

Synthesis

The three compounds $C_6F_5SiF_2CH_2NMe_2$ (**1**), $C_6F_5SiF_2N(SiMe_3)NMe_2$ (**2**) and $C_6F_5SiF_2ONMe_2$ (**3**) were prepared by

Fakultät für Chemie, Universität Bielefeld, Universitätsstrasse 25, 33615, Bielefeld, Germany. E-mail: mitzel@uni-bielefeld.de; Fax: +49 521 106 6029; Tel: +49 521 106 6163

† CCDC reference numbers 688419–688421. For crystallographic data in CIF or other electronic format see DOI: 10.1039/b808388f

similar procedures from $C_6F_5SiF_3$ with the respective lithiated reagents $LiONMe_2$, $LiN(SiMe_3)NMe_2$ and $LiCH_2NMe_2$ to yield the products by salt elimination.

$$C_6F_5SiF_3 + LiXNMe_2 \rightarrow C_6F_5SiF_2\text{–}X\text{–}NMe_2 + LiF$$
$$[X = CH_2\ (\mathbf{1}),\ N(SiMe_3)\ (\mathbf{2}),\ O\ (\mathbf{3})] \qquad (1)$$

Compound **1** is extremely hydrophilic and has to be strictly handled under inert gas. It can be crystallised at low temperatures from solution, but is a liquid at ambient temperature (mp –5 °C). Compound **2** can be recrystallised at low temperatures to give thin needles melting at 35 °C. All three compounds were identified and checked for purity by ^1H, ^{13}C, ^{19}F and ^{29}Si NMR (for **3**) and further characterised by IR and MS spectra.

Compound **3** can be crystallised from the melt by application of low-temperature *in situ* techniques (see below). It can be evaporated and transferred in a high vacuum line and this allowed measurements of a gas phase IR spectrum. Calculated vibrational spectra were derived from a force field obtained at the B3LYP/6-31G* level of theory. A comparison between calculated and measured spectra can be used to derive information about the conformation of the free molecules of **3**. In particular the region between 1200 and 700 cm^{-1} is very sensitive to the conformation of the molecules in this case as is shown in Fig. 1. A comparison with the calculations indicates strongly the predominant presence of the *gauche* conformer of **3** in the gas phase. The obtained simulation of the IR spectrum of the *gauche* conformer fits very well with the experimental spectrum as shown in Fig. 2. Comparison with the calculated spectra also suggests that some smaller bands, in particular those at 1538, 1078 and 1029 cm^{-1}, are likely to stem from the second, less abundant, *anti* conformer in the vapour phase.

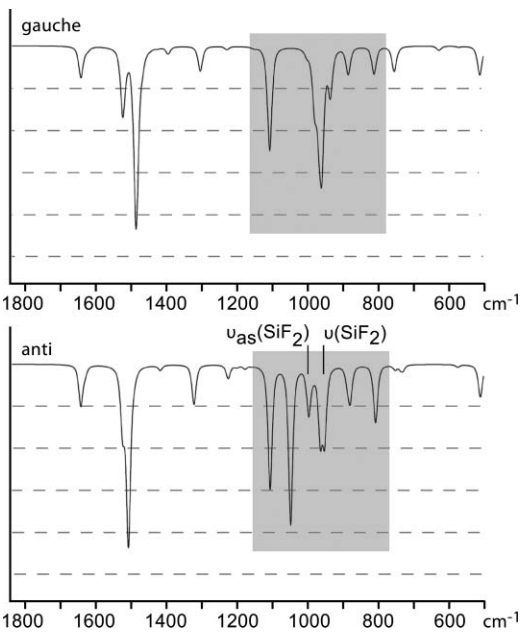

Fig. 1 Calculated (B3LYP/6-31G*) gas phase IR spectra in the region between 1800 and 500 cm^{-1} for the *anti* and *gauche* conformer of compound **3**.

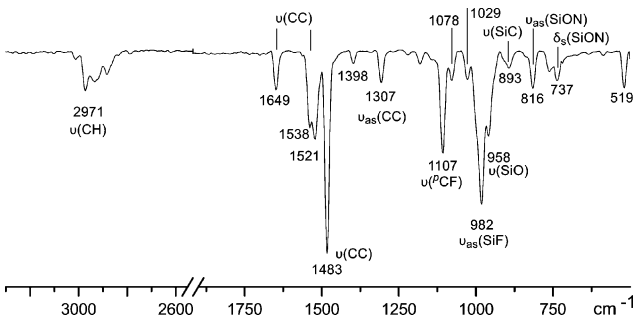

Fig. 2 Measured gas phase IR spectrum of compound **3**.

NMR spectroscopy

The signal for the NMe_2 group of **1** is found in the ^1H NMR spectrum at 2.32 ppm in C_6D_6 solution (compare: $F_3SiCH_2NMe_2$ 1.96 ppm).[16] In contrast, the corresponding resonances of compounds **2** (2.54 ppm) and **3** (2.68 ppm) are found at higher frequencies. Very similar in their chemical shifts are the ^{13}C NMR data (**1**: 49.4 ppm, **2**: 48.0 ppm, **3**: 49.5 ppm, $F_3SiCH_2NMe_2$: 48.5 ppm). This indicates that the electronic situation at the nitrogen donor centre is not very different for the three attached spacer groups in solution. The fluorine atoms at the acceptor atom Si also lead to surprisingly similar chemical shifts in the ^{19}F NMR spectra. Unfortunately we could not obtain meaningful ^{29}Si NMR spectra for **1** and **2**, probably owing to the weakness of the signals due to their multiple splitting by coupling to F nuclei. The ^{29}Si NMR shift of –48.3 ppm for **3** is between those of $Cl_3SiONMe_2$ and $H_3SiONMe_2$ (–42.4 ppm and 49.5 ppm).[4,5]

Molecular and crystal structures

Single crystals of compounds **1**, **2** and **3** were grown by three different methods: **1** by the OHCD-method[18] (optical heating and crystallisation device, a laser-assisted microscale zone-melting), **2** by crystallisation from solution and **3** by *in situ* methods from a solid–liquid equilibrium (Fig. 3, 4 and 5). The structural data are collected in Table 1 along with the results of *ab initio* calculations at the MP2/TZVPP level of theory.

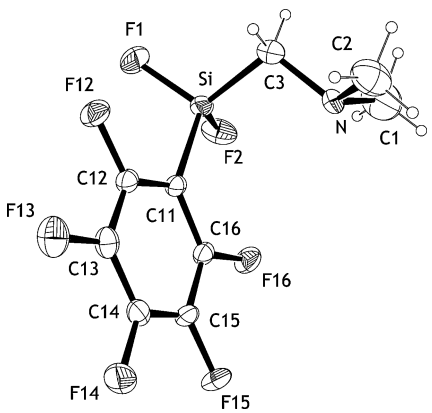

Fig. 3 Molecular structure of compound **1** in the crystal as obtained by low-temperature X-ray crystallography. The displacement factors are represented by ellipsoids at the 50% probability level.

All three compounds are monomeric in their crystals, which has an analogy in the related compounds $F_3SiXNMe_2$ for X = NR

Table 1 Selected bond lengths [Å], atom distances, angles [°] and torsion angles of $C_6F_5SiF_2$–X–NMe_2 [X = CH_2 (**1**), N($SiMe_3$) (**2**), O (**3**)] as determined by low temperature X-ray crystallography (XRD) and by *ab initio* calculations (MP2/TZVPP)

	1		**2**		**3**	
	XRD	MP2	XRD	MP2	XRD	MP2
d(Si–F_{anti})	1.569(3)	1.597	1.583(2)	1.606	1.580(3)	1.597
d(Si–F_{gauche})	1.540(4)	1.596	1.574(3)	1.598	1.576(2)	1.593
d(Si–X)	1.831(5)	1.867	1.660(3)	1.698	1.633(3)	1.662
d(X–N)	1.488(6)	1.460	1.494(5)	1.461	1.495(4)	1.481
d(Si···N)	2.676(4)	2.750	2.241(4)	2.230	2.117(3)	2.140
d(N–C1)	1.421(8)	1.454	1.461(5)	1.455	1.455(5)	1.455
d(N–C2)	1.445(8)	1.454	1.449(5)	1.456	1.466(5)	1.453
d(Si–C11)	1.868(4)	1.870	1.854(4)	1.872	1.857(4)	1.868
∠(Si–X–N) (α)	107.0(3)	110.8	90.4(2)	89.5	85.1(2)	85.6
∠(F–Si–X) (β)	108.6(2)	109.9	109.3(2)	109.4	103.4(2)	104.5
∠(C11–Si–X) (γ)	110.4(2)	109.8	115.8(2)	112.8	117.2(2)	115.6
τ(C11SiXN)	55.6(4)	29.4	65.5(2)	63.1	66.3	63.9
τ(lp_NNXSi)	26.5	47.3	3.1	2.4	1.7	2.1

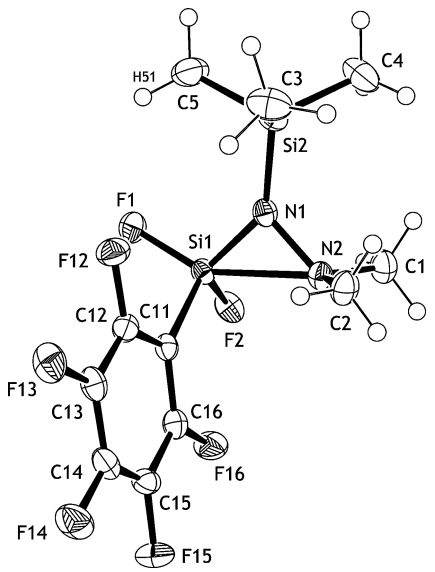

Fig. 4 Molecular structure of compound **2** in the crystal as obtained by low-temperature X-ray crystallography. The displacement factors are represented by ellipsoids at the 50% probability level.

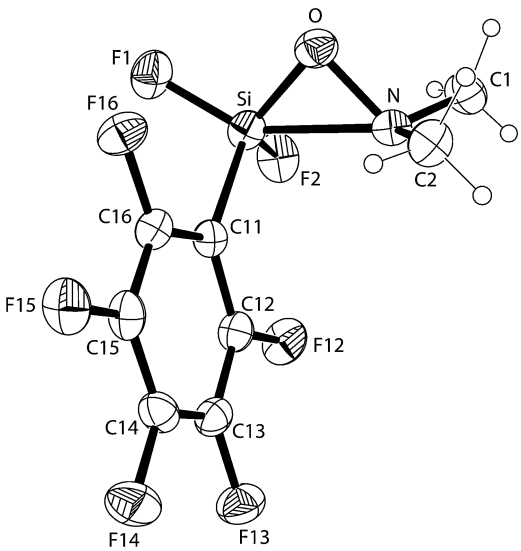

Fig. 5 Molecular structure of compound **3** in the crystal as obtained by low-temperature X-ray crystallography. The displacement factors are represented by ellipsoids at the 50% probability level.

and O, but is in variance to them for X = CH_2 ($F_3SiCH_2NMe_2$ is a dimer in the solid). Thus it is here for the first time that these situations can be compared directly with reliable data from the solid state. Moreover, all three compounds are found in the same conformation with the pentafluorophenyl group in *gauche* position [τ(C11SiXN) ≈ 60°], as was already indicated to be the most stable conformer in the gas phase. It is therefore the most electronegative substituent, fluorine, which is found in *anti* position relative to the Si–X–N skeleton—a situation that was not unexpected, as in a number of related cases different preferences were found.[11,12]

Whereas in the cases of **2** and **3**, the conformation of the NMe_2 group relative to the N–X–Si skeleton is such that these parts of the structures are almost of mirror symmetry, as is necessary for maximising the Si···N interactions, in compound **1** there is a marked deviation from such a conformation. As shown in Fig. 6 the position of a hypothetical lone pair (lp) of electrons at nitrogen (calculated as a vector enclosing three equal angles lp–N–C) deviates by 26.5° from an idealised position of the

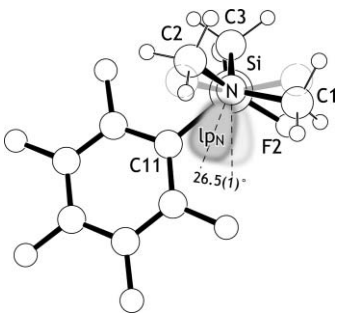

Fig. 6 View of compound **1** along the N–Si axis showing the orientation of the NMe_2 group relative to the SiCN plane. lp_N denotes the idealised position of the lone pair of electrons at the nitrogen atom and its deviation from a hypothetical orientation in the SiCN plane shown in faded print (including the corresponding hypothetical positions of the atoms of the NMe_2 group).

NMe_2 group, lying in the SiCN plane (by contrast, the lone pairs are approximately aligned in the SiON and SiNN planes

in compounds **2** and **3**). This leads to a substantial difference between the torsional angles Si–C–N–C to both Me groups being 94.1 and −144.3°. In contrast the corresponding torsional angles for compound **2** are 113.2 and −119.5° and for **3** they are 118.1 and −122.2°.

Comparing the backbone structures of compounds **1–3**, only the spacer group X (X = CH_2, $N(SiMe_3)$, O) varies and affects the Si···N interaction, which is structurally characterised by the Si–X–N angle and the Si···N distance. In the case of **1** the Si···N distance of 2.676(4) Å and the corresponding Si–C–N angle of 107.0(3)° are not indicative of an attractive Si···N interaction. A comparison of this angle determined in the solid state, *i.e.* in a polar surrounding of many molecules with relatively high dipole moments, with the situation of the free molecule described by the calculations shows a deviation of almost 4°, the largest deviation for the series **1–3**. These 107.0(3)° for the Si–C–N angle of **1** are, however, much smaller than the Si–C–N angle in the dimer of $F_3SiCH_2NMe_2$ (120.4 °).[16] We can also compare the structure of compound **1** with the zwitterionic ammoniomethyl(trifluorosilicate) $F_4SiCH_2NHMe_2$, which is not capable of forming a direct Si···N interaction due to the already hypercoordinate Si and tetracoordinate N atom. In this compound the Si–C–N angles are 118.5 and 119.2° for two independent molecules in the crystal.[19]

In contrast to **1** the other two compounds **2** and **3** have small Si–X–N angles [**2**: 90.4(2)°, **3**: 85.1(2)°], clearly indicating attractive Si···N interactions to be operative. This leads to relatively short Si···N distances of 2.241(4) Å and 2.117(2) Å, respectively. $C_6F_5Si(F)_2CH_2NMe_2$ (**1**) is the first SiCN compound for which no widened Si–C–N angle (bigger than the ideal 109.4°) is observed. This was the case for $F_3SiCH_2NMe_2$[16] with ∠(Si–C–N) = 110.3(7)° and for $H_3SiCH_2NMe_2$[17] with ∠(Si–C–N) = 114.7(3)° for which structures from the gas phase are available (gas electron diffraction).

In order to evaluate the possible influence of the electronic effect of substituents at the C atom of the SiCN linkage on the structures of such α-silanes, we calculated the structures of compounds of the type $R_3Si–C(R'')–NMe_2$. The results are compiled in Table 2 which shows that a contraction of the Si–C–N angle is possible when electropositive substituents are introduced. One or two trimethylsilyl groups at the spacer carbon atom in combination with electronegative substituents at silicon, F or F_5C_6, lead to such structures with small Si–C–N angles. The minimum among the investigated systems is predicted to be 83.5° for $(F_5C_6)F_2SiC(SiMe_3)_2NMe_2$. Interestingly this angle is more than two degrees smaller than in the trifluorosilyl compound $F_3SiC(SiMe_3)_2NMe_2$ (86.0°), which was unexpected, as

Table 2 Dependence of calculated SiCN angles on the substituents at the spacer carbon atom of the molecules $R_3Si–C(R'_2)–NMe_2$. Calculations are at the PBE/TZVPP(RI) level of theory, angles are given in °

	R'_2 =			
R_3 =	H_2	$(CH_3)_2$	$H(SiMe_3)$	$(SiMe_3)_2$
$(CH_3)_3$	116.8	109.1	105.3	105.4
H_3	114.6	108.7	104.9	110.7
F_3	113.1	107.8	102.7	86.0
$(F_5C_6)F_2$	113.9	107.0	88.9	83.5

the compounds with $SiNRNMe_2$ and $SiONMe_2$ units have smaller Si–N–N and Si–O–N angles for an F_3 rather than an $(F_5C_6)F_2$ substitution pattern at silicon.

The Si–N–N angle in **2** is 90.4(2)° and the Si···N distance is 2.241(4) Å. These values are much smaller than the corresponding ones in the aminomethylsilane **1**. *Ab initio* calculations at the MP2(RI)/TZVPP level of theory predicted this angle to be 89.5°, which is close to the crystal structure value. This angle is about seven degrees wider than in the trifluorosilyl compound $F_3SiN(SiMe_3)NMe_2$, but is equal to the one found in the *N*-trimethylstannyl substituted compound $F_3SiN(SnMe_3)NMe_2$ with 89.6°.[14]

In compound **2** the Si–N–Si angle is very wide at 140.7(2)° and marks the substantial deformation of the planar coordinate spacer nitrogen atom (sum of angles 359.5°). The C5-methyl group of the $SiMe_3$ unit is slightly bent towards the fluorine atom connected to the silicon in *anti* position relative to N, which results in a distance H51···F of about 2.60 Å. This interpretation of an attractive F···H interaction is supported by an N1–Si2–C5 angle of 104.6°, which is much smaller than the angles N1–Si2–C3 (111°) and <N1Si2C4 (112°), respectively. In contrast to **1** the orientation of the lone pair at the NMe_2 nitrogen (calculated idealised orientation) is oriented towards the silicon atom, as is described by a torsional angle lp_N–N1–N2–Si1 of 3.1°.

Likewise as in compound **1** and **2** the pentafluorophenyl group in **3** is placed in *gauche* position with a torsion angle τ(C11–Si–O–N) = 66.3(2)°. This was also predicted by *ab initio* calculations at a MP2(RI)/TZVPP level of theory. As expected, **3** shows the smallest Si–X–N angle [<SiON = 85.1(2)°] of all three pentafluorophenyl compounds in this paper. This Si–O–N angle is thus more than 5° smaller than the Si–N–N angle in **2** [<Si–N–N = 90.4(2)°] and 12° smaller than the Si–C–N angle in **3** [<Si–C–N = 107.0(3)°)] (see Fig. 4). Further structural parameter values are listed in Table 1.

We have already discussed the preference of the *gauche* conformers for compound **3** in the context of its IR spectrum (see above). In order to confirm this and to learn more about the energetics of conformations and structural changes between them, we have calculated a part of the potential surface by successive variation of the C11SiON and C11SiCN dihedral angles in **1** and **3** [PBE(RI)/TZVPP geometry optimization followed by single point energy calculations at the MP2(RI)/TZVPP level of theory]. Corresponding calculations for **2** have not been undertaken for reasons of computational feasibility, and because **1** and **3** mark both extremes for the presence and absence of Si···N attractive interactions. Fig. 7 shows the MP2 energies of **1** and **3** as a function of both the C11–Si–C–N (C11–Si–O–N) dihedral angle and the Si–C–N (Si–O–N) bending angle for **1** (**3**) in the forms of three-dimensional perspective plots. The highest barrier to the transition between *gauche* to *anti* position of the C_6F_5 group in **1** is about 14 kJ mol^{-1}, whereas it is almost twice as high for **3** with 26 kJ mol^{-1}. The transition between both *gauche* positions is lower for both compounds and is 6 kJ mol^{-1} for **1** and more than twice as high for **3** at 16 kJ mol^{-1}. Whereas the barriers are lower for **1**, the absolute energy differences between *gauche* and *anti* conformers is higher for **1** with 8 kJ mol^{-1}, while **3** has a corresponding energy difference of about 6 kJ mol^{-1}. Nevertheless, the *gauche* conformer is the preferred for both compounds. Thus the reason why only *gauche* conformers are observed in the crystal structures and for **3**

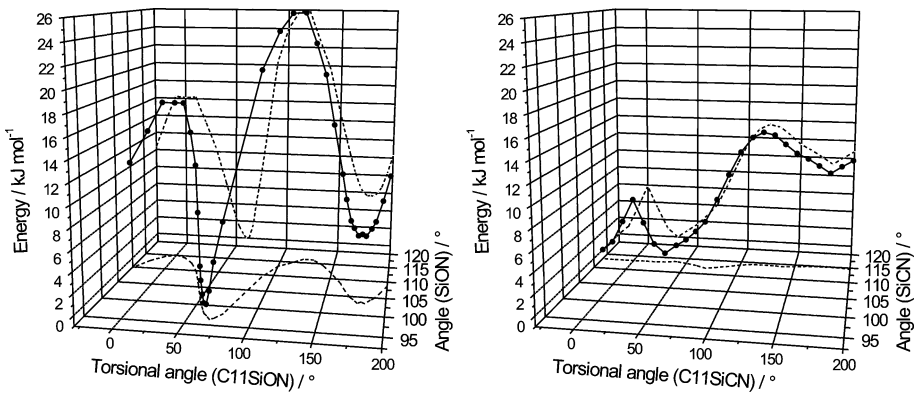

Fig. 7 Dependence of the energy and angle SiXN (X = C, O) on the conformation/torsional angle C11SiXN in compounds **1** (left) and **3** (right). For better comparison, the axes are drawn on the same scale. The plots are shown as a three-dimensional graph representing the individual calculation points with projections into two dimensions showing a dependence angle on torsion (bottom) and energy/torsion (back). Calculations were performed as single point calculations (MP2/TZVPP) based on relaxed geometries with restricted torsional angles (PBE/TZVPP).

in the gas phase is clearly an inherent property and not forced by intermolecular forces in the solid state.

It is also interesting to observe the angles Si–C–N and Si–O–N during the rotation of the silyl group about the Si–C and Si–O bonds, respectively. The Si–C–N angle in the case of **1** varies over a range of only a few degrees during such a rotation, whereas the corresponding Si–O–N angle in **3** changes by about 20° during a full rotation. This indicates also, that in **3** certain orientations of the silyl group only allow for an interaction with the geminal N atom, which is an argument against purely electrostatic interaction and in favour of orientationally dependent orbital interactions like a negative hyperconjugation of the type lp(N)→σ*(Si–X). However, it has to be mentioned that we have already investigated the latter possibility in terms of the electron density topologies and could not find evidence for this for other SiON systems, but found indications in favour of lp(N)→σ*(Si–F) interactions in $F_3SiONMe_2$ or lp(N)→σ*(Si–Cl) interactions in $ClH_2SiONMe_2$ by means of NBO analyses.[11,12] $ClH_2SiONMe_2$ is also a nice example for which the orientation dependence of the electronegative substituents at silicon becomes manifest, as the *anti* conformer (with the Cl atom in the SiON plane) has a much stronger Si···N attractive interaction than the *gauche* conformer, in which a less electron withdrawing H atom is in *anti* position relative to the nitrogen atom.

Experimental

General

All reactions were carried out under an atmosphere of dry nitrogen in anhydrous and degassed solvents with standard Schlenk and high vacuum techniques. NMR spectra were recorded on AC200, Avance 400 or Varian Inova 500 spectrometers in deuteriated solvents and were referenced relative to (residual) solvent resonances (^{1}H, ^{13}C, ^{19}F) or relative to an external standard (^{29}Si; neat $SiMe_4$). Infrared spectra were measured on a Midac Prospect-IR spectrometer. Mass spectra were recorded on a Varian MAT 212 or on a Pfeiffer QMG422/SEM.

Syntheses

$F_6C_5SiF_2CH_2NMe_2$ (1). A suspension of 0.15 g (2.31 mmol) *N*,*N*-dimethylaminomethyllithium in 20 mL dry pentane was added dropwise from a funnel equipped with a magnetic stirrer into a solution of $C_6F_5SiF_3$ (0.64 g, 2.54 mmol) in pentane (10 mL) at −50 °C. After allowing warming to −30 °C during $\frac{1}{2}$ h, the reaction was completed by stirring for 2 h at this temperature. Then the suspension was filtered through a glass wool filter fitted to a PTFE cannula and the residue was washed with 2 × 5 mL pentane. The volume was reduced by one third. Storing at a temperature of −78 °C led to precipitation of the product. Yield: 0.15 g, 0.52 mmol, 22%, mp −5 °C. ^{1}H NMR ($CDCl_3$; 200 MHz): δ 2.32 ppm (s, 6 H, $(CH_3)_2$), 2.40 (s, 2 H, CH_2), ^{13}C NMR ($CDCl_3$; 50.3 MHz): δ 46.4 ppm (s, CH_2), 49.4 (s, $N(CH_3)_2$). 125.0 (m, CF_3, $^1J(C,F) = 317$ Hz). ^{19}F NMR ($CDCl_3$, 188.3 MHz): δ −158.9 ppm (*m*-F), −145.3 (*p*-F, $^3J_{F,F} = 20$ Hz), −133.8 (t, SiF, $^1J_{Si,F} = 126$ Hz), −126.5 (*o*-F). IR(gas) 518 (m) ν(SiC), 730 (w) ν(SiCH2), 755 (vw), 812 (w) $\rho(CH_2)$, 890 (s) ν(SiF), 941 (s) ν_{as}(SiF), 977 (vs) ν_{as}(CF), 1042 (w) $\rho(NCH_2)$, 1103 (vs) ν(pCF), 1157 (vw) $\tau(SiH_2)$, 1180 (vw) $\omega(SiH_2)$, 1251 (w) $\delta(CH_2)$, 1305 (s) ν(CF), 1390 (s) ν(CC), 1483 (vs) δ_{as}(CC), 1521 (vs), 1650 (s), 2780–2989 (w) ν(CH). MS (EI) *m*/*z* (%) 291 (M^+, 92), 289 (M^+ − 2H, 100), 123 ($M^+ - C_6F_5$, 3.8), 57 (NMe_3 − 2H, 6).

$C_5F_6SiF_2N(SiMe_3)NMe_2$ (2). A solution of 0.48 g (3.5 mmol) *N*-lithio-*N*-trimethylsilyl-*N*′,*N*′-dimethylhydrazine (generated from *N*-trimethylsilyl-*N*′,*N*′-dimethylhydrazine[20] and *n*-butyllithium) in 10 mL dry pentane was added dropwise to a solution of 0.97 g (3.85 mmol) trifluoro-pentafluorophenylsilane in 15 mL dry pentane at −40 °C. After allowing warming to ambient temperature over 2 h the mixture was filtered through a glass wool fitted PTFE cannula and washed two times with 5 mL pentane. After reducing the volume by one half the product precipitated at −78 °C over night in the form of fine clear crystalline needles, which are sensitive to moisture. Yield: 1.10 g, 3.02 mmol, 86%, mp 35 °C. ^{1}H NMR (C_6D_6; 200 MHz): δ = 0.29 ppm (s, 9H, $Si(CH_3)_3$), 2.54 ppm (s, 6 H, $(CH_3)_2$), ^{13}C NMR (C_6D_6; 50.3 MHz): δ = 2.0 ppm (s, $Si(CH_3)_3$), 48.0 (s, $N(CH_3)_2$).

125.0 (m, C_6F_5), ^{19}F NMR ($CDCl_3$, 188.3 MHz): $\delta = -160.7$ ppm (*m*-F), −149.2 (*p*-F, $^3J_{F,F} = 21$ Hz), −133.9 (t, SiF, $^1J_{Si,F} = 175$ Hz), −127.0 (*o*-F). IR(gas) = 508 (s), 700 (m), 760 (m), 809 (s) $\rho(CH_3)$, 841 (s), 904 (s) ν(SiF), 974 (s) ν_{as}(SiF), 1021 (m), 1080 (bs) ν(SiN), 1173 (m), 1230 (m), 1259 (s), 1291 (m), 1388, 1473, 1516, 2789–2964 (w) ν(CH). MS (EI) [*m*/*z*(%)]: 364 (M^+, 100%), 349 ($M^+ - CH_3$, 30%), 257 ($M^+ - F - CH_3 - SiMe_3$, 26%), 233 ($M^+ - NSiMe_3$)NMe_2, 7%), 168 (C_6F_5H, 12%), 73 ($SiMe_3$, 83%).

$F_6C_5SiF_2ONMe_2$ (3). 1.26 g (5.00 mmol) of trifluoropentafluorophenylsilane were condensed onto a suspension of an excess of diethyl ether and 0.34 g (5.0 mmol) *O*-lithio-*N*,*N*-dimethylhydroxylamine. After warming to RT and stirring for 3 h the mixture was filtered through a glass wool filter fitted to a PTFE cannula. The solvent and remaining $C_6F_5SiF_3$ were removed under reduced pressure until the residue became oily. Some remaining LiF precipitated by addition of 10 mL dry hexane. After filtration the vessel was cooled to −10 °C and the solvent was completely removed under reduced pressure to give **3** as a colourless liquid. Yield: 0.76 g, 2.9 mmol, 48%, mp 10 °C. ^{1}H NMR ($CDCl_3$; 400 MHz): $\delta = 2.68$ ppm (s, 6 H, $(CH_3)_2$). ^{13}C NMR ($CDCl_3$; 100.6 MHz): $\delta = 49.5$ ppm (s, NCH_2), 100.0 (s, C_{ipso}). 149.3–137.3 (m, C_6F_5), ^{19}F NMR ($CDCl_3$, 376.5 Hz): $\delta = -159.2$ ppm (*m*-F), −145.9 (*p*-F), −133.8 (t, SiF, $^1J_{Si,F} = 126$ Hz), −126.9 (*o*-F). ^{29}Si NMR: ($CDCl_3$; 79.5 MHz). $\delta = -48.3$ ppm. IR(gas) = 518 (m) ν(SiC), 735 (w), 816 (w), 959 (s) ν(SiF), 982 (s) ν_{as}(SiF), 1109 (vs) (ρCF), 1308 (s) ν(CF), 1399 (s) ν(CC), 1483 (vs), 1522 (vs), 1649 (s), 2876–2977 (w) ν (CH). MS (EI) [*m*/*z*(%)]: 293 (M^+, 0.2%), 168 (C_6F_5H, 81%), 148 ($Si(ONMe_2)_2$, 100%), 126 ($M^+ - C_6F_5$, 20%).

Crystal structures

The experimental setup for low temperature crystal growth of **1** consists of an X-ray diffractometer (Stoë IPDS 1) with an attached nitrogen cryostream. An IR-laser source is set up in such a way that the sample can be heated with the focused laser-beam. The intensity and position of the laser focus is computer controlled. The liquid samples were added to thin-walled glass capillaries (approx. 0.25 mm inner diameter) and were then sealed. After placing a capillary on the goniometer head, the sample was cooled to *ca.* 20 K below the melting point (polycrystalline solidification). The IR laser (hitting a tiny portion of *ca.* 0.2 mm of the capillary) was then applied at an intensity sufficient to partially melt the polycrystalline compound. It was then scanned 4 times along the length of the capillary very slowly (approx. 2.5 mm h^{-1}) at −50 °C. During this procedure the temperature was kept constant. After starting at the bottom (0%) of the capillary the next turn will be started at a position of 10% of the scanning range. The last run was started at 40% and ended at 100%. After finishing the crystallisation procedure a suitable single crystal can be identified by means of a microscope equipped with a polarisation filter.

A crystal of **3** was grown on a CAD4 diffractometer with cryostream from a seed crystal, which was selected in a carefully established solid–liquid equilibrium, by melting other crystals followed by slowly lowering the temperature until the whole capillary was filled with a single crystal.

The structures were solved by direct methods and refined using standard crystallographic software.[21] Non-hydrogen atoms of all structures were refined with anisotropic displacement parameters. Hydrogen atoms were included in calculated positions and refined with a riding model with fixed angles and distances for **1**, with group-wise refining distances and fixed angles for **2** and located in difference Fourier maps and refined with isotropic displacement parameters for **3**. See Table 3 for crystal and refinement data.

Table 3 Crystal and refinement data for the crystal structures of **1–3**

Compound	**1**	**2**	**3**
Formula	$C_9H_8F_7NSi$	$C_{11}H_{15}F_7N_2Si_2$	$C_8H_6F_7NOSi$
Formula weight	291.25	364.41	293.23
Crystal system	Triclinic	Orthorhombic	Orthorhombic
Space group	$P\bar{1}$	$Pna2_1$	$P2_12_12_1$
Diffractometer	STOE IPDS I	Bruker APEX	Nonius CAD4
a/Å	5.897(1)	28.767(11)	6.325(1)
b/Å	10.362(2)	8.542(3)	10.809(1)
c/Å	10.892(2)	6.264(2)	15.633(2)
α/°	68.54(3)	90	90
β/°	80.39(3)	90	90
γ/°	74.53(3)	90	90
V/Å^3	593.1(2)	1539.2(10)	1068.8(2)
ρ_{calc}/g cm^{-3}	1.631	1.573	1.822
Z	2	4	4
μ/mm^{-1}	1.113	0.913	1.033
T/K	213(2)	153(2)	143(2)
Index range	$-6 \le h \le 6$ $-12 \le k \le 12$ $-13 \le l \le 13$	$-40 \le h \le 40$ $-12 \le k \le 12$ $-8 \le l \le 8$	$-0 \le h \le 8$ $-17 \le k \le 17$ $-20 \le l \le 5$
$2\vartheta_{max}$/°	51.65	60.08	54.30
Measured refl.	7718	17049	3503
Unique refl.	5631	4448	2320
Observed refl.	2020	2893	1793
R_{int}	0.123	0.252	0.072
Parameters	165	224	188
Absolute strucure parameter		0.2(2)	0.0(3)
$R[I > 2\sigma(I)]/wR_2$	0.081/0.179	0.085/0.151	0.050/0.118
R[all refl]/wR_2	0.096/0.190	0.106/0.156	0.080/0.131
$\rho_{fin(max/min)}$/e Å^{-3}	0.74/−0.31	1.05/−0.33	0.44/−0.36

Conclusions

With the series of compounds $C_6F_5SiF_2CH_2NMe_2$ (**1**), $C_6F_5SiF_2N(SiMe_3)NMe_2$ (**2**) and $C_6F_5SiF_2ONMe_2$ (**3**) we have for the first time a set of α-donor-functionalised silanes with identical donor and acceptor functions separated by different spacer units CH_2, $N(SiMe_3)$ and O, which are all monomeric in the solid state (in the series $F_3SiCH_2NMe_2$, $F_3SiNRNMe_2$ and $F_3SiONMe_2$ such a comparison was impossible due to the fact that $F_3SiCH_2NMe_2$ dimerises, whereas the other two compounds are monomeric in the crystalline phase). This allowed a comparison of their structures in this phase. Only for **2** and **3** are there clearly attractive structure-determining interactions between the geminal Si and N atoms, as indicated by their Si–X–N angles [**2**: 90.4(2) and **3**: 85.1(2)°]. $C_6F_5SiF_2CH_2NMe_2$ (**1**), in contrast, has an Si–C–N angle of 107.0(3)°, which shows that—if at all—only extremely weak attractive forces are present. This is also supported by the potential curves for the rotation about the Si–X axes for **1** and **3**, which show a strong dependence of the Si···N distance and Si–O–N angle on the orientation of the $F_5C_6F_2Si$ group, whereas these parameters are not very much affected by rotating this group about the Si–C axis in **1**.

Acknowledgements

This work was supported by the Deutsche Forschungsgemeinschaft. We are grateful to Tania Pape for collecting the crystallographic data for compound **2** and to Dr Alexander Hepp for NMR measurements.

Notes and references

1 (*a*) R. G. Kostyanovskii and A. K. Prokov'ev, *Dokl. Akad. Nauk SSSR*, 1965, **164**, 1054; (*b*) V. V. Kharpov, V. I. Gol'danskii, A. K. Prokov'ev and R. G. Kostyanovskii, *Zh. Obshch. Khim.*, 1967, **37**, 3; (*c*) E. W. Randall, C. H. Yoder and J. J. Zuckerman, *Inorg. Chem.*, 1967, **6**, 744; (*d*) Z. Pacl, M. Jakoubkova, Z. Papouskova and V. Chvalovsky, *Collect. Czech. Chem. Commun.*, 1971, **36**, 1588; (*e*) A. Marchand, J. Mendelsohn, M. Lebedeff and J. Valade, *J. Organomet. Chem.*, 1969, **17**, 379.

2 M. A. Brook, *Silicon in Organic, Organometallic and Polymer Chemistry*, John Wiley & Sons, New York, 2000, p. 500.

3 (*a*) G. Mital and R. R. Gupta, *J. Am. Chem. Soc.*, 1969, **91**, 4664; (*b*) J. M. Bellama and A. G. MacDiarmid, *J. Organomet. Chem.*, 1970, **24**, 91; (*c*) N. Egorochkin, S. E. Skobeleva, E. I. Sevast'yanova, I. G. Kosolapova, V. D. Sheludyakov, E. S. Rodionov and A. D. Kirilin, *Zh. Obshch. Khim.*, 1976, **46**, 1795.

4 (*a*) W. K. Musker and G. K. Larson, *J. Organomet. Chem.*, 1966, **6**, 627; (*b*) M. E. Freeburger and L. Spialter, *J. Am. Chem. Soc.*, 1971, **93**, 1894.

5 L. G. L. Ward and A. G. MacDiarmid, *J. Inorg. Nucl. Chem.*, 1961, **20**, 345.

6 (*a*) N. F. Lazareva, E. I. Brodskaya and G. V. Ratovsky, *J. Chem. Soc., Perkin Trans. 2*, 2002, 2083; (*b*) N. F. Lazareva, V. P. Baryshok and M. G. Voronkov, *Russ. Chem. Bull.*, 1995, **104**, 374; (*c*) D. Labreque, K. T. New and T. H. Chan, *Organometallics*, 1994, **13**, 332.

7 (*a*) A. Bauer, T. Kammel, B. Pachaly, O. Schäfer, W. Schindler, V. Stanjek and J. Weis, in *Organosilicon, Chemistry V*, Wiley-VCH, Weinheim, 2003, p. 527; (*b*) *One step ahead – organofunctional silanes from Wacker*, Brochure of the Wacker company: http://www.wacker.com/internet/webcache/de_DE/BrochureOrder/GENIOSIL_Brosch_e.pdf; (*c*) W. Schindler, *Adhaes.–Kleben Dichten*, 2004, **48**, 29.

8 (*a*) N. W. Mitzel, A. J. Blake and D. W. H. Rankin, *J. Am. Chem. Soc.*, 1997, **119**, 4143; (*b*) N. W. Mitzel and U. Losehand, *Angew. Chem.*, 1997, **109**, 2897, (*Angew. Chem., Int. Ed. Engl.*, 1997, **36**, 2807); (*c*) U. Losehand and N. W. Mitzel, *Inorg. Chem.*, 1998, **37**, 3175; (*d*) N. W. Mitzel and U. Losehand, *Eur. J. Inorg. Chem.*, 1998, 2023; (*e*) N. W. Mitzel, U. Losehand and A. D. Richardson, *Inorg. Chem.*, 1999, **38**, 5323; (*f*) N. W. Mitzel, U. Losehand and D. W. H. Rankin, *J. Chem. Soc., Dalton Trans.*, 1999, 4291; (*g*) N. W. Mitzel, U. Losehand and B. Bauer, *Inorg. Chem.*, 2000, **39**, 1998; (*h*) U. Losehand and N. W. Mitzel, *J. Chem. Soc., Dalton Trans.*, 2000, 1049; (*i*) N. W. Mitzel, U. Losehand, S. L. Hinchley and D. W. H. Rankin, *Inorg. Chem.*, 2001, **40**, 661; (*j*) N. W. Mitzel and U. Losehand, *Z. Naturforsch., B: Chem. Sci.*, 2001, **56**, 630; (*k*) N. W. Mitzel and K. Vojinovic, *J. Chem. Soc., Dalton Trans.*, 2002, 2341; (*l*) K. Vojinović, N. W. Mitzel, T. Foerster and D. W. H. Rankin, *Z. Naturforsch., B: Chem. Sci.*, 2004, **59**, 1505.

9 U. Losehand and N. W. Mitzel, *J. Chem. Soc., Dalton Trans.*, 1998, 2537.

10 (*a*) N. W. Mitzel, H. Schmidbaur, D. W. H. Rankin, B. A. Smart, M. Hofmann and P. v. R. Schleyer, *Inorg. Chem.*, 1997, **36**, 4360; (*b*) N. W. Mitzel, *Chem.–Eur. J.*, 1998, **4**, 692.

11 N. W. Mitzel and U. Losehand, *J. Am. Chem. Soc.*, 1998, **120**, 7320.

12 N. W. Mitzel, U. Losehand, A. Wu, D. Cremer and D. W. H. Rankin, *J. Am. Chem. Soc.*, 2000, **112**, 4471.

13 N. W. Mitzel, K. Vojinović, R. Fröhlich, T. Foerster and D. W. H. Rankin, *J. Am. Chem. Soc.*, 2005, **127**, 13705.

14 K. Vojinović, L. McLachlan, D. W. H. Rankin and N. W. Mitzel, *Chem.–Eur. J.*, 2004, **10**, 3033.

15 K. Vojinović, N. W. Mitzel, M. Korth, R. Fröhlich and S. Grimme, in *Organosilicon Chemistry VI*, ed. N. Auner and J. Weis,Wiley VCH, Weinheim, 2005, vol. 1, pp. 156–159.

16 N. W. Mitzel, K. Vojinović, T. Foerster, H. E. Robertson, K. B. Borisenko and D. W. H. Rankin, *Chem.–Eur. J.*, 2005, **11**, 5114.

17 N. W. Mitzel, C. Kiener and D. W. H. Rankin, *Organometallics*, 1999, **18**, 3437.

18 R. Boese, M. Nussbaumer, *In situ* Crystallization Techniques, in *Correlations, Transformations, and Interactions in Organic Crystal Chemistry, IUCr Crystallographic Symposia*, ed. D. W. Jones and A. Katrusiak, Oxford University Press, Oxford, UK, 1994, vol. 7, p. 20–37.

19 R. Tacke, J. Becht, O. Dannappel, R. Ahlrichs, U. Schneider, W. S. Sheldrick, J. Hahn and F. Kiesgen, *Organometallics*, 1996, **15**, 2060.

20 U. Wannagat and F. Hoefler, *Monatsh. Chem.*, 1966, **97**, 976.

21 (*a*) G. M. Sheldrick, *Acta Crystallogr., Sect. A: Found. Crystallogr.*, 1990, **46**, 467; (*b*) G. M. Sheldrick, Universität Göttingen, Germany, 1997.

